two-body potentials, viz., (a) the inclusion of successive physical effects through suitable additions in the potentials, and (b) different algebraic forms of parametrization for the various potentials. In particular, we have presented new results with "analytic" potential shapes, whose main interest derives from the exact interpretation it can provide for the parameter β as an exchanged mass, in terms of more conventional ideas of field theory. The preliminary results with such single-rank potentials are very encouraging for the BE as well as for $a_{1/2}$ (when one remembers the oscillatory variation of $a_{1/2}$ between negative and positive values as the strength parameter changes). This fact encourages the hope that a more elaborate analytic potential (including noncentral terms), each term of which can be interpreted to arise from the exchange of a meson of appropriate mass and quantum numbers, may find useful applications to the three-body problem so as to provide a better *raison d'être* for such calculations from the point of view of theory.

The analytic potentials seem to yield significantly different results for $a_{1/2}$ and BE than the corresponding Yamaguchi and Yukawa potentials of rank-2. While it may be premature from a comparison of such simple potentials to make any quick inference on the genuineness of the effect of shape variations on three-body parameters, this feature seems to persist even in a comparison of more elaborate potentials (including core terms), which agree much more closely on the energy shell.

This sensitivity of three-body parameters to the choice of potential shapes may be interpreted as bringing out the important role of N-N correlations in a $3N$ system which are (in a way) a direct manifestation of the off-shell effects in the N-N potential. This sensitivity also represents the main limitation against the assignment of quantitative physical significance to the results of $3N$ calculations with *assumed* N-N potentials, since any ambiguity in the shape of the latter will reflect directly on the results of $3N$ calculations.

Such an unenviable situation would remain unavoidable as long as N-N interactions remain at their present empirical level. Perhaps a partial answer in principle lies in the consideration of more formal meson-theoretic potentials[47] which should preferably be put directly into the generalized Faddeev framework which consists of a set of coupled two-dimensional integral equations. The feasibility of such a program, however, looks quite remote with the present-day machine sizes and speeds. Under such circumstances, three-body investigations with simplified potentials would presumably retain some usefulness, but the physical limitations of its scope must be recognized as quite severe. In particular, a disagreement of $\sim$1 MeV in the value of the BE should by no means be regarded as significant, and perhaps even a wider latitude should be allowed to $a_{1/2}$ in view of its smallness and greater sensitivity. Judged in this light, it is perhaps a fortunate coincidence that the simplest Yamaguchi parametrization with the inclusion of tensor and core effects seems to be consistent with both BE and $a_{1/2}$, while several other forms of parametrization fail to bring out even this qualitative result.

ACKNOWLEDGMENT

The authors are grateful to Mrs. Sharon Schrenk (formerly of the Temple University Computer Center) for generous help with many of the computational problems associated with this investigation.

[47] e.g., R. Bryan and B. L. Scott, Phys. Rev. **135**, B434 (1964).

PHYSICAL REVIEW C VOLUME 1, NUMBER 3 MARCH 1970

Elastic Neutron-Alpha Scattering Analyses*

Richard A. Arndt and L. David Roper
Virginia Polytechnic Institute, Blacksburg, Virginia 24061
(Received 29 October 1969)

An energy-dependent phase-shift analysis of 0–20-MeV n-α scattering is attempted. Reasonable fits to the 0–16.4 data are obtained, but the rest of the data up to 20 MeV elude good fits. Single-energy analyses at energies where polarization data are available corroborate the energy-dependent analysis. Our results differ from the Hoop-Barschall phases as follows: $P_{1/2}$ is larger between 3 and 10 MeV; $S_{1/2}$ and $P_{3/2}$ are larger between 10 and 16.4 MeV. We are not able to reliably determine D or F waves in this energy range.

I. INTRODUCTION

A CONVENIENT way to study the five-nucleon problem is to study p-α and n-α scattering. Of course, p-α scattering experiments are much easier to perform than are n-α experiments, because the proton has charge whereas the neutron does not. One expects p-α and n-α scattering to be almost identical, owing to charge independence of the strong interaction. However, near sharp resonances and thresholds, where the scat-

* Work supported in part by the U.S. Atomic Energy Commission and a grant from the National Science Foundation.

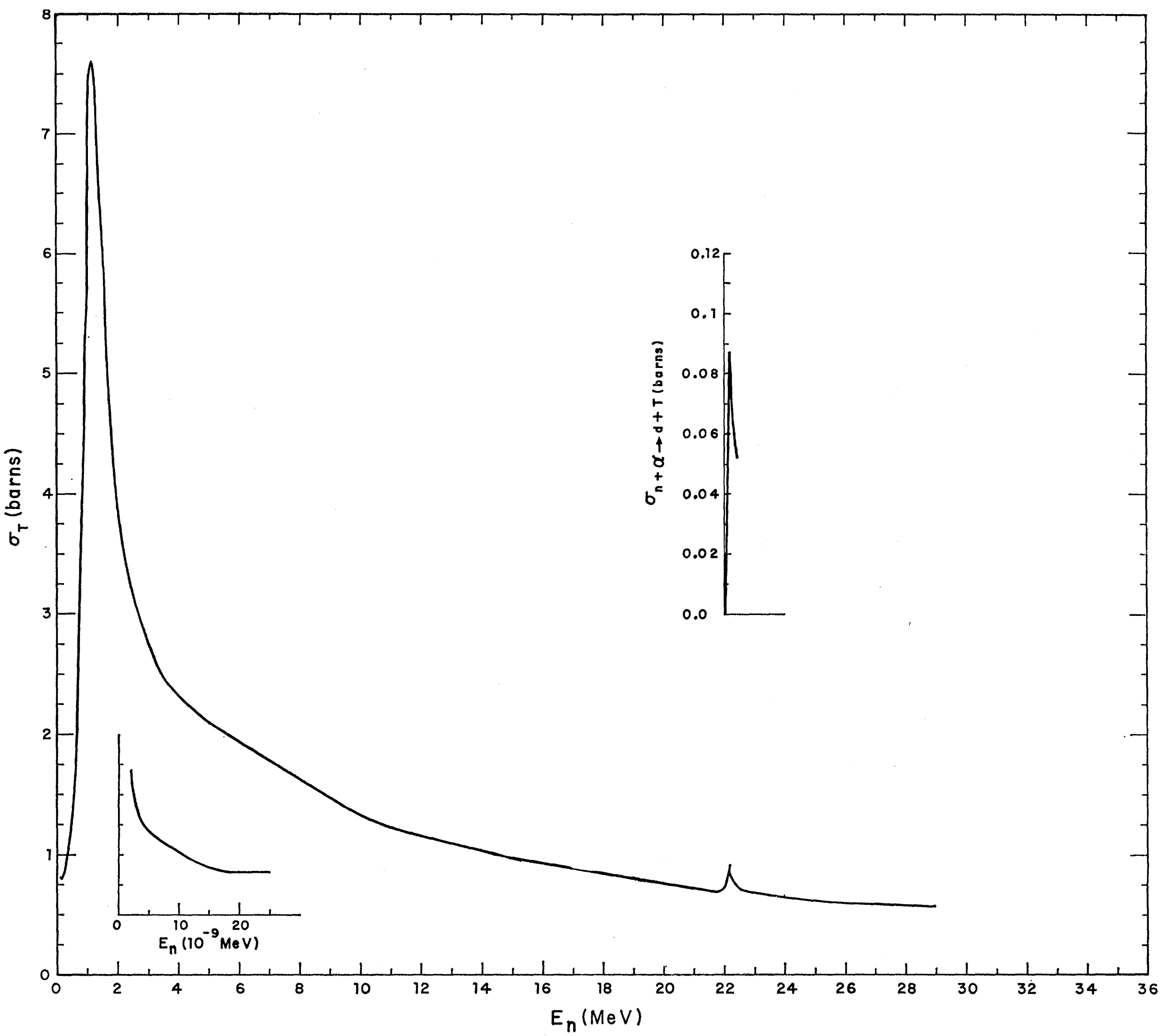

FIG. 1. Visual curve for the $n-\alpha$ total cross section σ_T and the $n+\alpha\to d+t$ reaction cross section.

tering partial waves vary rapidly, the small mass difference may be important. The p-α scattering data have been analyzed extensively,[1] but clarifications are still needed. In this report, we concentrate on the analysis of the n-α scattering data. Further, we consider only n-α elastic scattering (laboratory neutron energy $= E_n < 22.06$ MeV $=$ the $n+\alpha\to d+T$ threshold).

Large amounts of n-α scattering data have recently been measured.[2] Some of these data have been separately partial-wave analyzed by the groups who measured them. We put all of the data together into an energy-dependent partial-wave analysis as well as analyze them separately at single energies where polarization data are available. An extensive set of differential cross-section measurements were made by Hoop and Barschall[3] (HB). They used their data to piece together partial waves with a rather involved prescription, but apparently did not perform a full computer analysis of the data. The recently determined phase shifts agree fairly well with each other except for the $P_{1/2}$ state. (Compare HB and recent Duke phases[4] in Figure 5.) We use the HB partial waves as one possible input in our full computer analysis. We obtain another input by using the Duke $P_{1/2}$ phases instead of the HB $P_{1/2}$ phases. Also, other inputs are tried.

Our energy-dependent solution (0–16.4 MeV) differs from HB in the $P_{1/2}$ state from 3 to 10 MeV, and in the $S_{1/2}$ and $P_{3/2}$ states from 10 to 16 MeV. Our best single-

[1] A. C. L. Barnard, C. M. Jones, and J. L. Weil, Nucl. Phys. **50**, 604 (1964); W. G. Weitkamp and W. Haeberli, *ibid.* **83**, 46 (1966); D. J. Plummer, T. A. Hodges, K. Ramavataram, D. G. Montague, and N. S. Chant, *ibid.* **A115**, 253 (1968); D. Garreta, J. Sura, and A. Tarrats, *ibid.* **A132**, 204 (1969).

[2] See the Appendix for Refs. D13, D14, D15, P7, and P8.

[3] See Ref. D13 in the Appendix.

[4] See Refs. D14 and P7 in the Appendix.

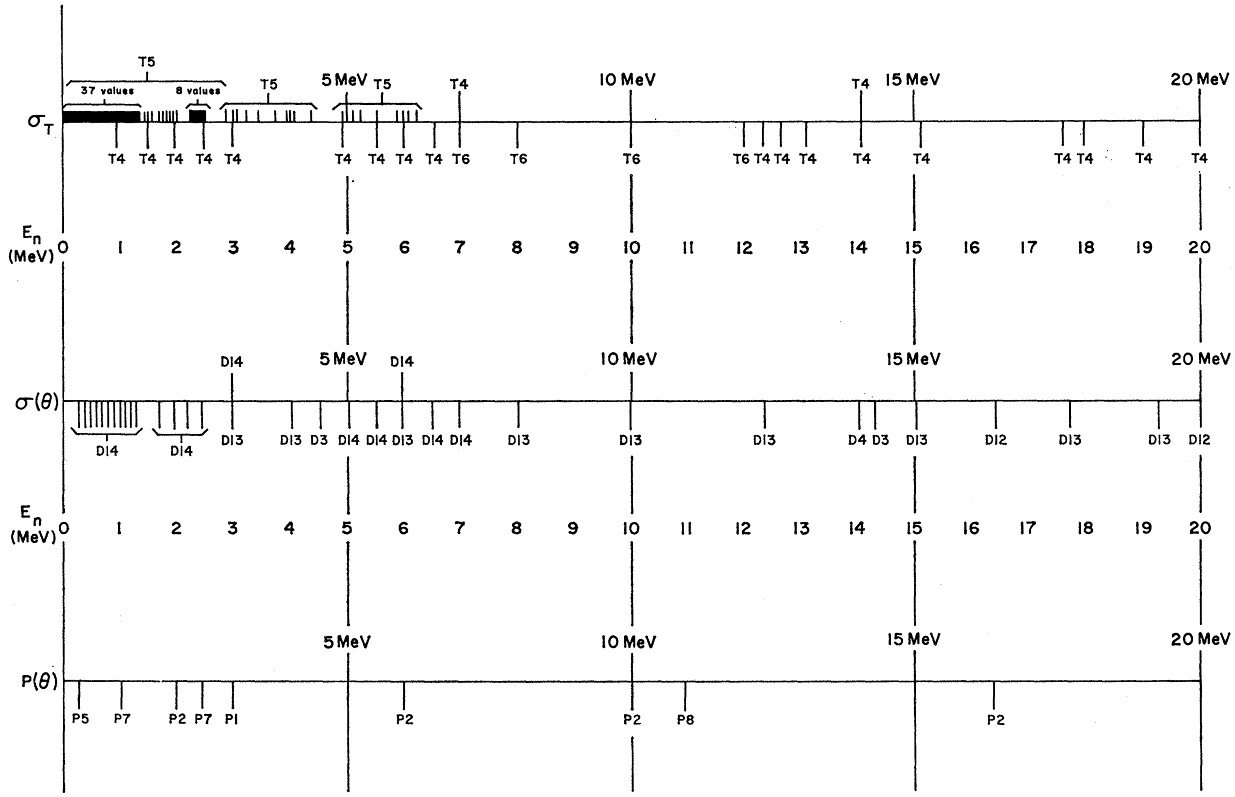

FIG. 2. Energies where σ_T, $\sigma(\theta)$, and $P(\theta)$ measurements have been made.

energy results agree with the energy-dependent result except at 12 MeV and 16 MeV (see Fig. 7).

II. DATA

In spin-0–spin-$\frac{1}{2}$ scattering, there are four angular observables[5] at each energy:

(1) $\sigma(\theta)$—differential cross section,
(2) $P(\theta)$—recoil spin-$\frac{1}{2}$ particle polarization,
(3) $R(\theta)$
(4) $A(\theta)$ —spin rotation parameters.

To date no one has measured $R(\theta)$ and $A(\theta)$ for any spin-0–spin-$\frac{1}{2}$ system.

For n-α scattering, many measurements of $\sigma(\theta)$ and about a dozen of $P(\theta)$ have been made.

Besides the angular observables there are total cross sections σ_T and inelastic reaction cross sections σ_r for the various possible reactions. To date there are many values of σ_T up to 30 MeV and a few values scattered at higher energies. The only reaction cross sections available are $\alpha(n, d)T$ from threshold (22.06 MeV) to 22.4 MeV. Some of these are obtained by applying detailed balance to the cross sections for the $T(d, n)\alpha$ reaction.

Figure 1 shows a rough curve for σ_T and σ_r for $n+\alpha\rightarrow d+T$. The large peak due to the $P_{3/2}$ resonance is the dominant feature. The broadening of this peak at the high-energy end is due to the large $P_{1/2}$ phase shift. The general background due to the $S_{1/2}$ phase shift and the $D_{3/2}$ resonance peak at 22.16 MeV are easily seen.

Figure 2 shows the energies where σ_T, $\sigma(\theta)$, and $P(\theta)$ measurements have been made. The greatest obvious need for data revealed by Fig. 1 and 2 is for more of $P(\theta)$ between 21 and 23 MeV around the $D_{3/2}$ resonance at 22.16 MeV and the inelastic threshold at 22.06 MeV. Also, from 30 MeV on up, data of all kinds are needed. Later we shall comment on needed measurements in the elastic region ($E_n<22$ MeV).

III. DATA SELECTION

In collections of experimental scattering data there are always redundancies and inconsistencies. In a system where the detected particle is neutral, as in the n-α system, the inconsistencies are enhanced. It is incumbent upon the analyzer of scattering data to cull out "bad data" and redundant data.

Inconsistent data are most safely culled by simultaneously considering all of the data over the selected energy range, and culling out those experiments that are obviously inconsistent with the entire body of data. This is done before an analysis begins or very early in the analysis. Later in the analysis, as unique solutions are (hopefully) obtained, these solutions can be cautiously used to point out finer inconsistencies in the

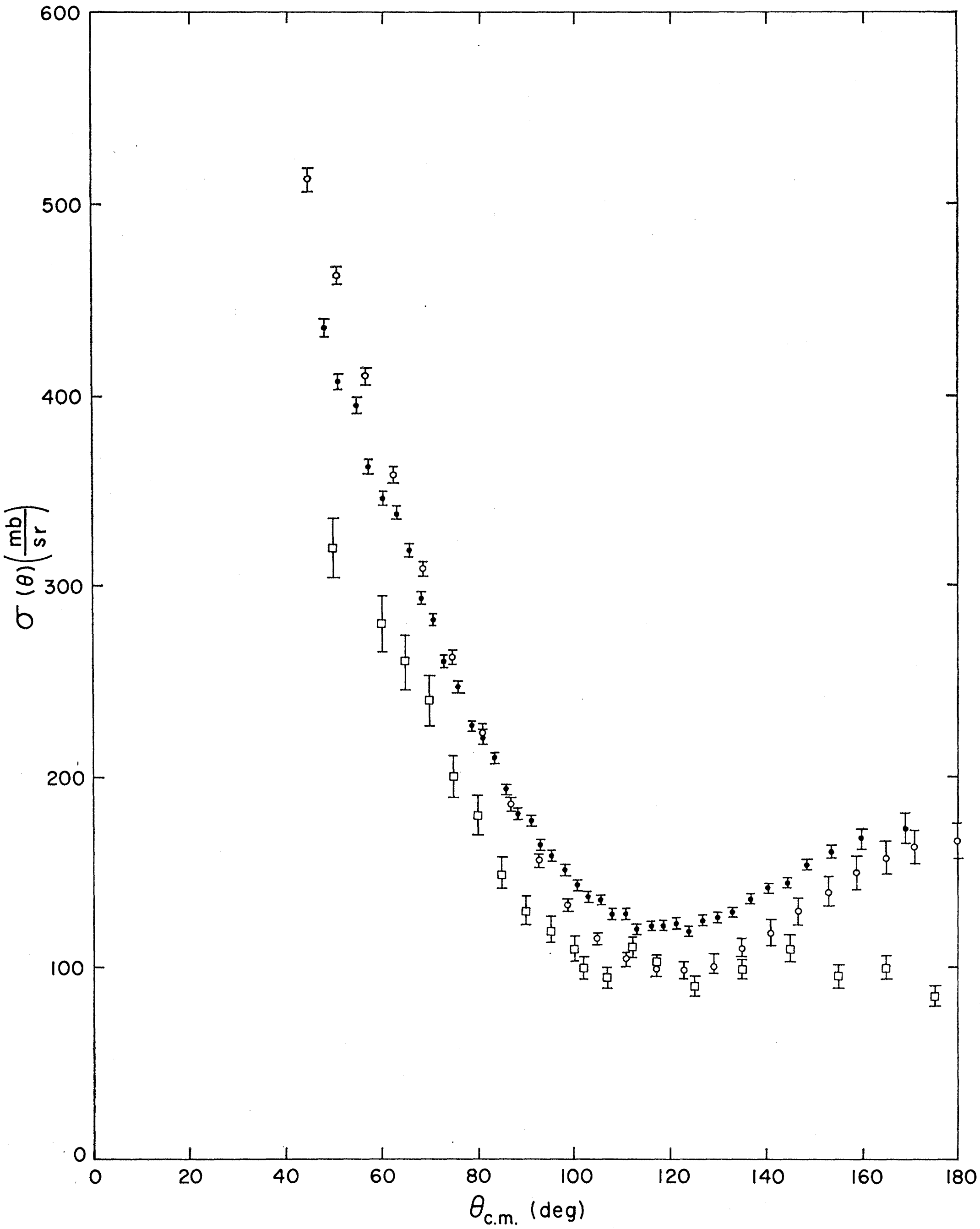

FIG. 3. An example of the inconsistencies among the data. ● = Duke data (Ref. D14) at 2.454 MeV. ○ = Italy data (Ref. D8) at 2.37 MeV. □ = Adair data (Ref. D1) at 2.4 MeV.

data. Ideally, these fine inconsistencies should be checked out by further experimental measurements.

Careful reading of experimental papers and communications with the experimentalists are indispensible in culling out redundant data. A few general rules are applicable with caution.

(1) Experimentalists often report preliminary data which is later superceded by their final data; (2) new data generally should have preference over old data; and (3) more precise data generally should have precedence over less precise data. We now apply the above principles and cull the elastic n-α scattering data.

A. Total Cross Section

Inconsistencies are abundant among the total cross-section data. Applying the principles given above we

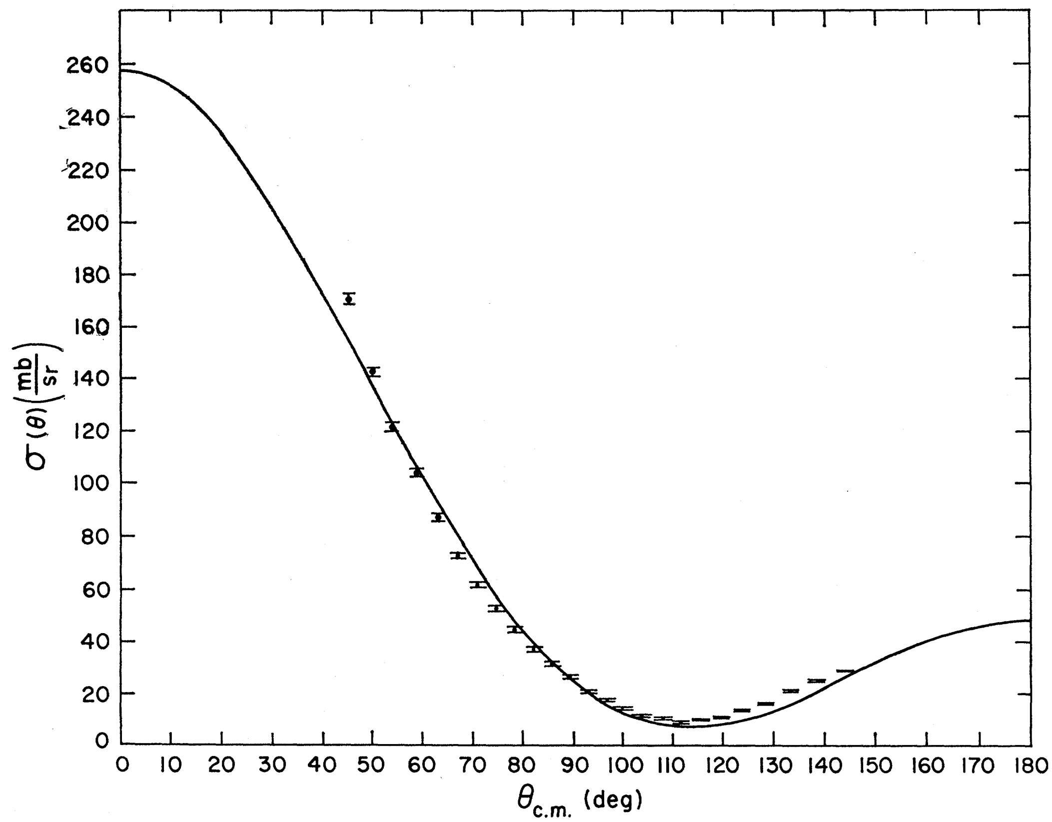

FIG. 4. Differential cross-section curve calculated at 18 MeV from HB phases (Ref. D13) compared to the 17.74-MeV HB data.

reduce the number of σ_T data to 96 from about twice that number. There still are serious inconsistencies which we cannot resolve among the selected data. Thus, we do not expect statistically good χ^2's in our least-squares fits to the data.

B. Differential Cross Sections

The most recent measurements (D12, D13, D14, D15 in the Appendix) are much more consistent with each other than they are with most of the earlier measurements. Also, the earlier measurements are not consistent with each other. An example of these inconsistencies is shown in Fig. 3.

In particular, the first-published Adair data (data Ref. D1) greatly disagree with later measurements at angles nearest 180°. Recent measurements have been made near all of the energies measured by Adair. Therefore, we discard all of the Adair data.

The 1962, Italy data (D8) at 2.37 and 2.87 MeV disagree with the late Wisconsin data (D13) at 3.02 MeV and Duke data (D14) at 2.454 and 2.98 MeV. We discard the Italy data.

The 1963 Padova data (D11) at 14.1 disagrees with the measurements at 14.1 MeV by Smith (D4) and at 14.3 MeV by Seagrave (D3). We discard the Padova data.

The 1953 Seagrave data (D3) at 2.61 MeV, when compared to recent surrounding data, appears to be too low at angles greater than 90°. The rest of the Seagrave data are consistent with more recent data. However, more precise data are available at all of the energies measured by Seagrave except 4.53 and 14.3 MeV. Therefore, we discard all Seagrave data except at 4.53 and 14.3 MeV.

There are discrepancies among the Wisconsin data (D13) at 2.02 MeV and the Duke data (D14) at 1.961 MeV. The Wisconsin data do not agree with the Hoop-Barschall (Wisconsin) phase shifts, but the Duke data do agree. We discard the Wisconsin data at 2.02 MeV.

C. Polarization

There are very few polarization data (see the Appendix). We hesitate to discard any. However, the one value at 3 MeV and 90° (P1) appears quite inconsistent with the values at 2 MeV (P2), 2.44 MeV (P7), and 6 MeV (P2). We discard it.

It should be noted that the polarizations reported by May *et al.* (P2) are given in terms of the laboratory scattering angle. We converted the laboratory angles to c.m. angles.

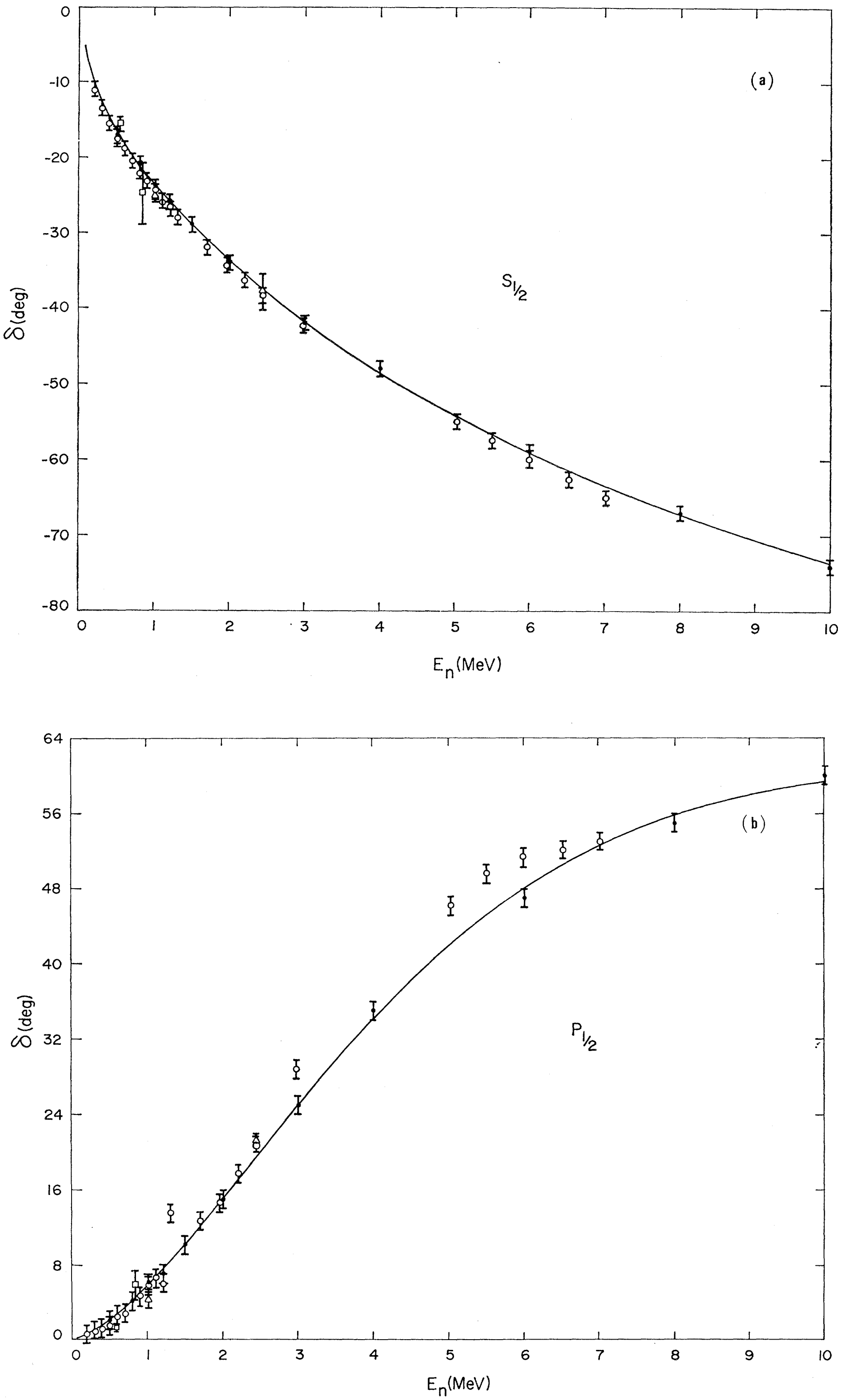

FIG. 5. *s*- and *p*-wave phase shifts from 0 to 10 MeV. The curves are our fits to the HB phases (Ref. D13); ○ = Duke (Morgan) phases (Ref. D14), △ = Duke (Sawers) phases (Ref. P7), □ = Virginia phases (Ref. D15), ● = HB phases (Ref. D13). We used errors of 1° on the HB phases.

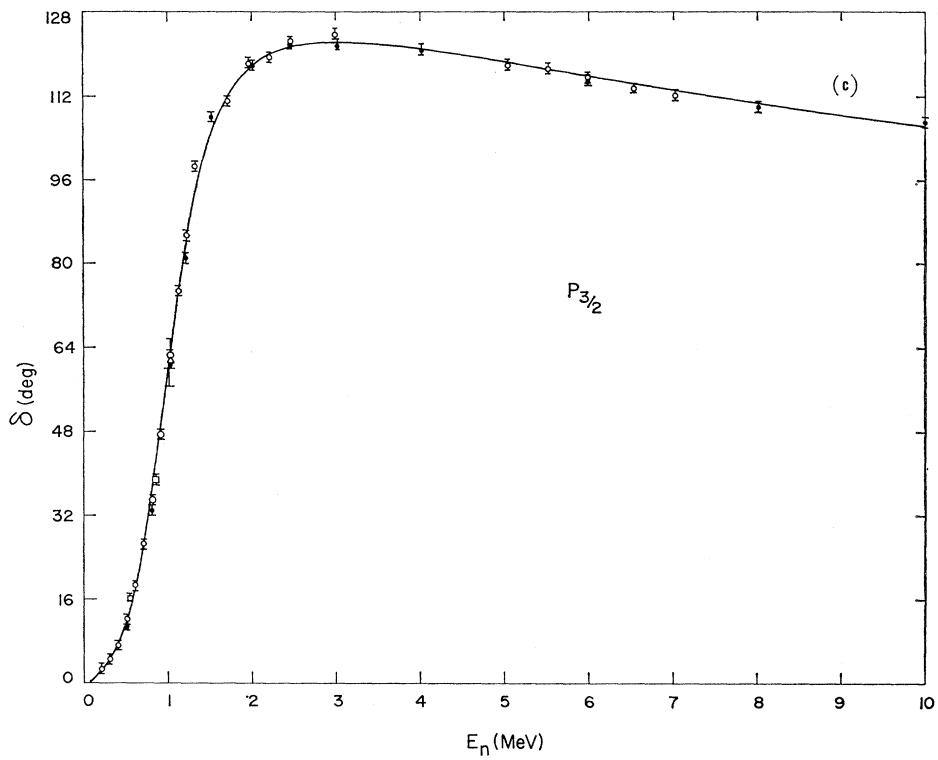

FIG. 5 (*Continued*)

IV. ENERGY PARAMETERIZATION AND LEAST-SQUARES FIT

We use the single-channel special case of a multichannel effective-range parameterization that we have developed for particle scattering analyses. The parameterization for the phase shift δ_l is

$$\rho \operatorname{ctn}\delta_l = \sum_m \gamma_m E_n{}^m,$$

where l = orbital angular momentum, the phase space factor $\rho = k^{2l+1}$, k = nonrelativistic relative momentum=

TABLE I. Energy-dependent parameters for fits to 0–20-MeV HB phase shifts.

l_{2J}	n	γ_n	No. of data	No. of parameters	χ^2_{expt}[a]	χ^2[b]
S_1	0	−0.8647	16	3	13	2.4
	1	0.06579				
	2	−0.001221				
P_1	0	0.4066	16	4	12	3.6
	1	0.02905				
	2	−0.002447				
	3	0.0003553				
P_3	0	0.1281	16	4	12	23.6
	1	−0.1094				
	2	0.006794				
	3	−0.0001130				
D_3	0	140.8	16	1	15	0.91
D_5	0	67.69	16	1	15	0.89
F_5	0	774.8	16	1	15	0.51
F_7	0	708.2	16	1	15	0.47
		Totals:	112	15	97	32.4

[a] Expected $\chi^2 = \chi^2_{\text{expt}}$ = No. of data − No. of parameters.

[b] We used errors of 1° on the HB phases.

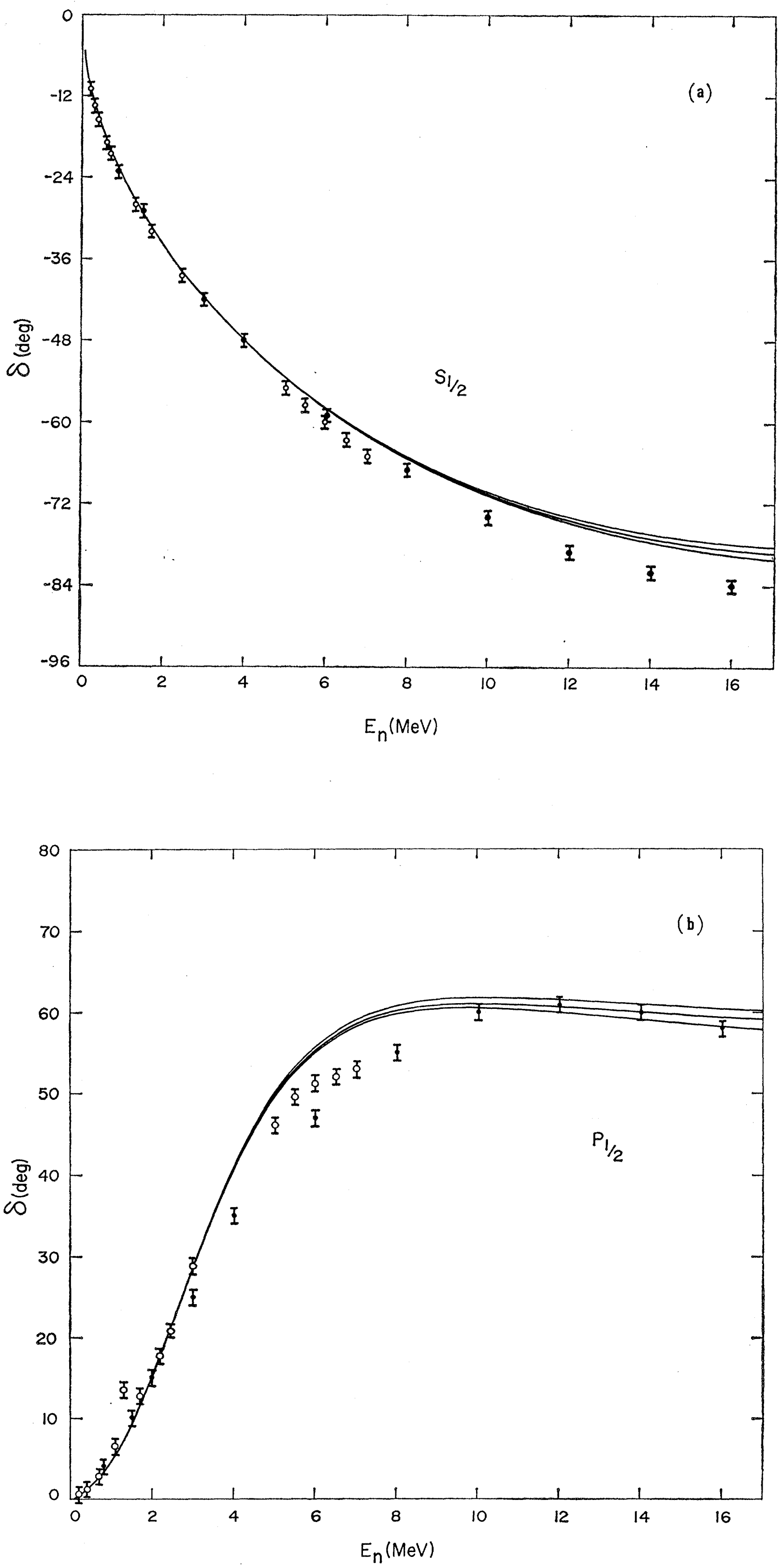

FIG. 6. Solution 11 of Table III and some of the HB and Duke phases. The data points are as in Fig. 5.

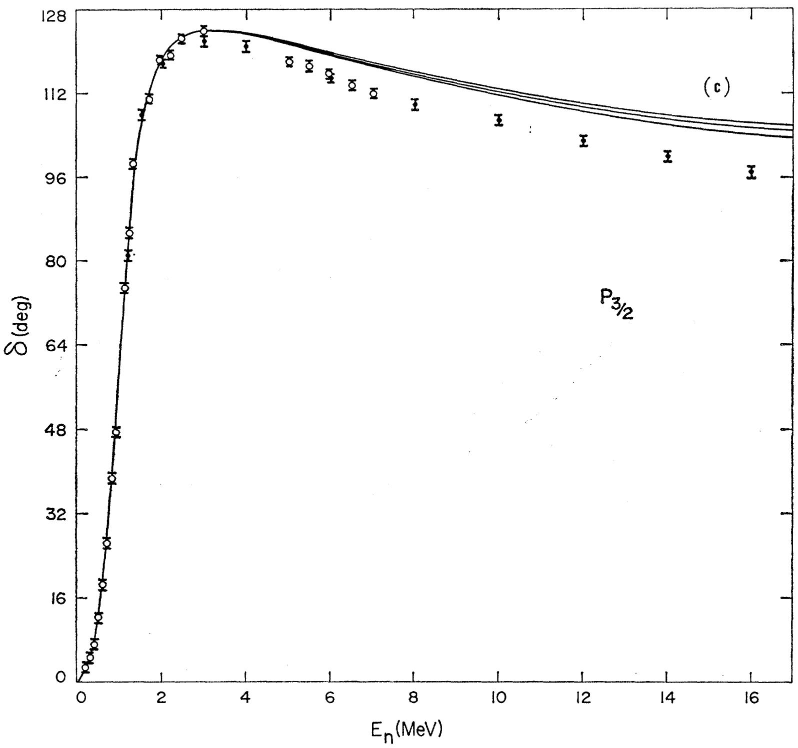

FIG. 6 (*Continued*)

$\frac{1}{2}$ (c.m. momentum), and γ_m are coefficients to be varied to fit the data. The neutron laboratory kinetic energy is E_n. We use inverse Fermi as the unit for k and MeV as the unit for E_n.

Many kinds of elastic phase-shift behavior can be represented by this parameterization. A notable exception is a zero in the phase shift. To allow for this possibility one would have to add a pole term to the expansion:

$$\rho \operatorname{ctn}\delta_l = \sum_m \gamma_m E_n^m + \beta/(E_n - E_0),$$

where E_0 is the energy position of the zero desired.

The equations relating the phase shifts to the observables are given in Ref. 5. The least-square search

TABLE II. Four different input $P_{1/2}$ phase behaviors and corresponding energy-dependent parameters.

Input name: E_n (MeV)	HB	HB2	HB3	Duke[a]	Duke-HB[a]
6	47°	47°	47°	51.3°	51.3°
10	60	61	59	53	60
16	58	76	67	46	58
20	54	85	70	40	54
Parameters					
γ_0	0.4066	0.2982	0.4560	0.5492	0.46936
γ_1	0.02905	0.03925	−0.01339	−0.0898	−0.03715
γ_2	−0.002447	0.003622	0.007012	0.01404	0.007276
γ_3	0.0003553	−0.0002822	−0.0002029		
χ^2	3.63	27.0	1.89	38.7	46.0
No. of data points	16	16	16	28	28

[a] The $P_{1/2}$ phase shifts below 7 MeV are taken from Ref. 4. Above 7 MeV the assumed behavior is as indicated here. The point at 1.306 MeV is inconsistent with the surrounding points (see Fig. 5). It alone gives almost one-half of the χ^2 value. All other input phase shifts are HB when this $P_{1/2}$ phase-shift behavior is used as input in the analysis.

[5] L. D. Roper, R. M. Wright, and B. T. Feld, Phys. Rev. **138,** B190 (1965); L. D. Roper and R. M. Wright, *ibid.* **138,** B921 (1965); L. D. Roper and D. S. Bailey, *ibid.* **155,** 1744 (1967).

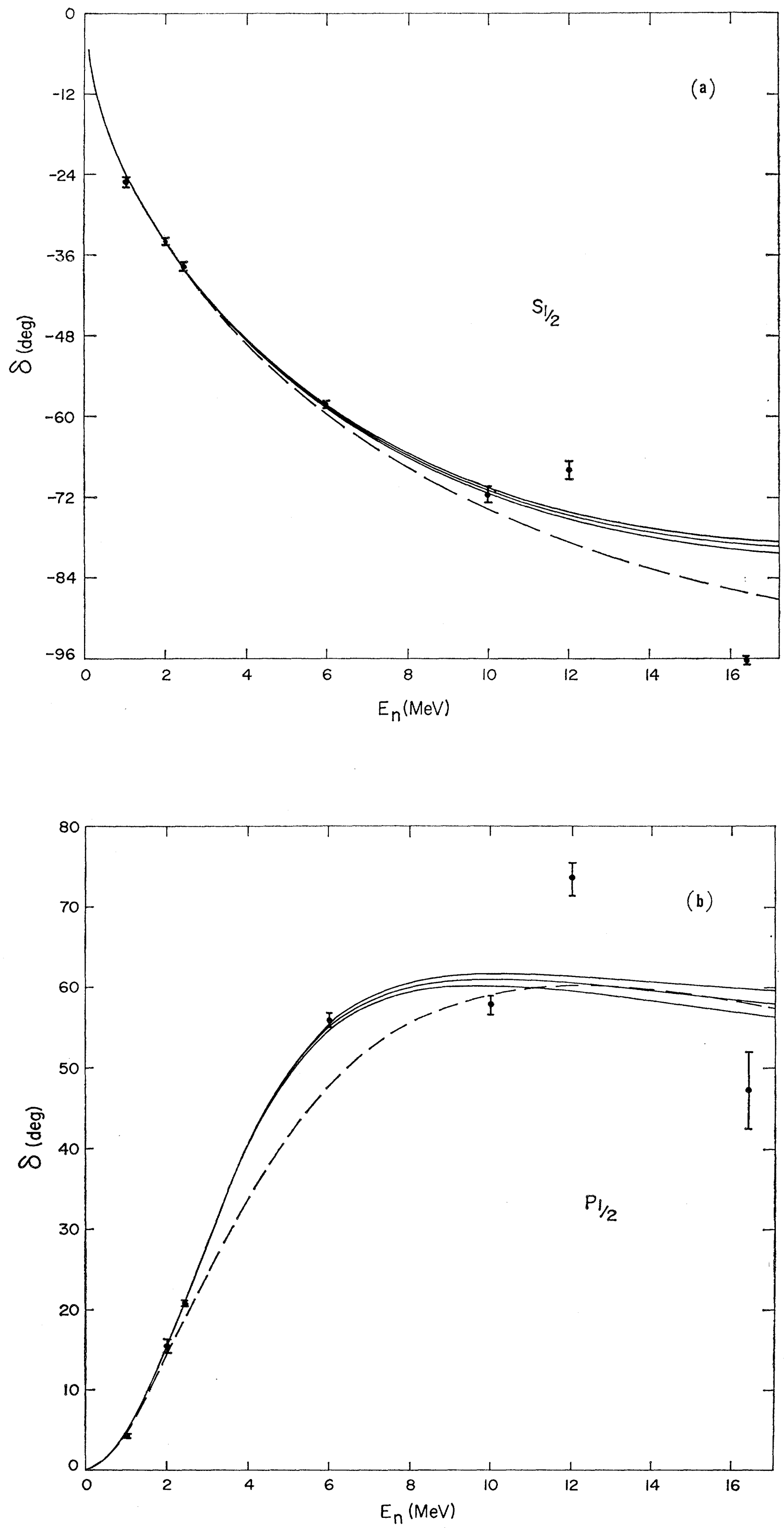

FIG. 7. Solution 18 of Table III (Solid curves), HB input (dashed curves), and the best single-energy results in Table V.

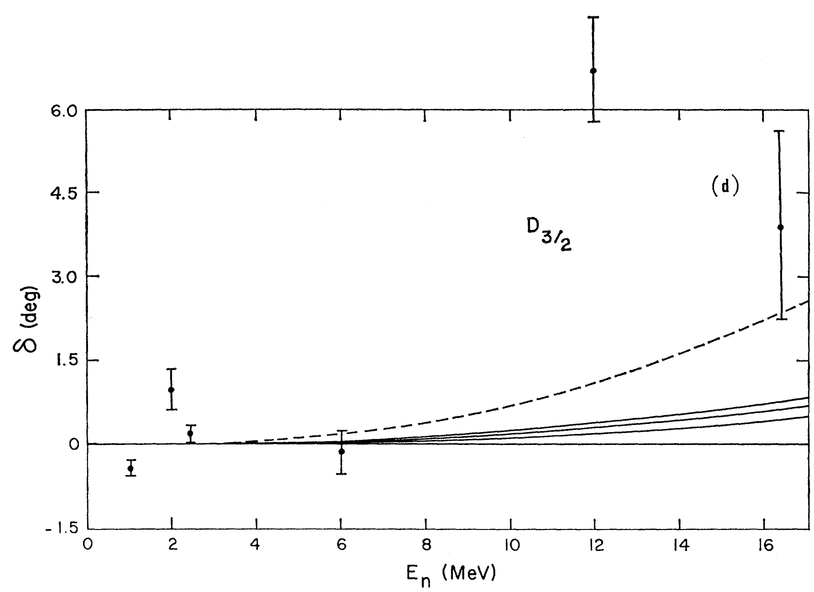

FIG. 7 (*Continued*)

procedure is given in Ref. 6. No corrections are included for the very small interaction between the neutron magnetic moment and the α-particle charge.

[6] R. A. Arndt and M. H. MacGregor, Meth. Comp. Phys. 6, 253 (1966).

V. INPUT PARAMETERS

We wish to try several sets of input parameters to test for uniqueness. One input set is obtained by fitting the HB single-energy phase shifts[3] from 0 to 20 MeV by our energy-dependent parameterization. The HB

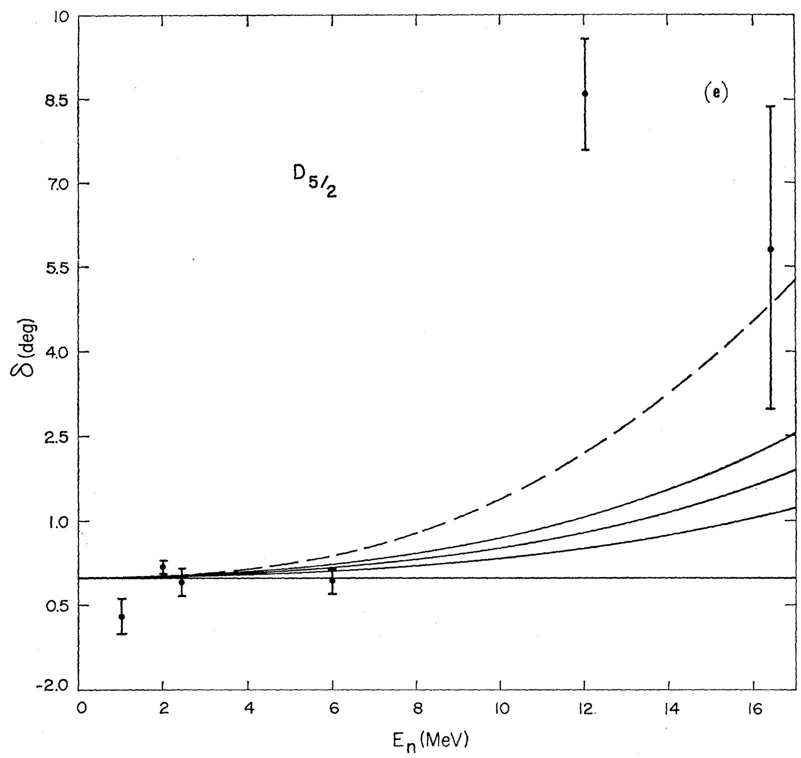

FIG. 7 (*Continued*)

TABLE III. 0–16.4-MeV energy-dependent fits.

Solution No.	No. of data	Input	Phases searched	No. of parameters	Expected χ^2	χ^2	$\chi^2/\chi^2_{\rm expt}$	Special features of result
1	1411	HB	SPDF	15	1396	2995	2.12	$D_{3/2}$ small, $F_{5/2}$ searches to 0
2	1411	HB2	SPDF	15	1396	2760	1.98	$D_{3/2}<D_{5/2}<0$
3	1411	HB3	SPDF	15	1396	2860	2.05	$0<D_{3/2}<D_{5/2}$
4	1411	Duke	SPDF	14	1397	2924	2.10	$D_{3/2}$ and $D_{5/2}$ small, $F_{5/2}$ large
5	1411	Sol. 2 (HB2)	SPD	13	1398	2698	1.93	Little change from sol. 2
6	1411	Sol. 3 (HB2)	SPD	13	1398	2800	2.01	Little change from sol. 3
7	1411	Sol. 5 (HB2)	$SPD_{3/2}$	12	1399	2694	1.93	Little change from sol. 6
8	1411	Sol. 6 (HB3)	$SPD_{5/2}$	12	1399	2794	2.00	Little change from sol. 7
9	1411	Sol. 7 (HB2)	SP	11	1400	2696	1.93	
10	1411	Sol. 8 (HB3)	SP	11	1400	2765	1.98	
11	1394	Sol. 9 (HB2)	SP	11	1383	2447	1.77	Almost identical solutions
12	1394	Sol. 10 (HB2)	SP	11	1383	2472	1.79	(see Fig. 6)
13	1394	Sol. 5 (HB2)	SPD	13	1381	2447	1.77	$D_{3/2}<D_{5/2}<0$
14	1394	Sol. 6 (HB3)	SPD	13	1381	2516	1.82	$0<D_{3/2}<D_{5/2}$
15	1394	HB	SP	11	1383	2742	1.98	
16	1394	Sol. 15	SPDF	15	1379	2705	1.96	
17	1415	HB	SPDF	15	1379	2705	1.98	
18	1415	HB2	SPDF	15	1400	2580	1.86	$0<D_{3/2}<D_{5/2}$
19	1415	HB3	SPDF	15	1400	2584	1.87	$0<D_{3/2}<D_{5/2}$
20	1415	Duke-HB	SPDF	14	1401	3015	2.15	

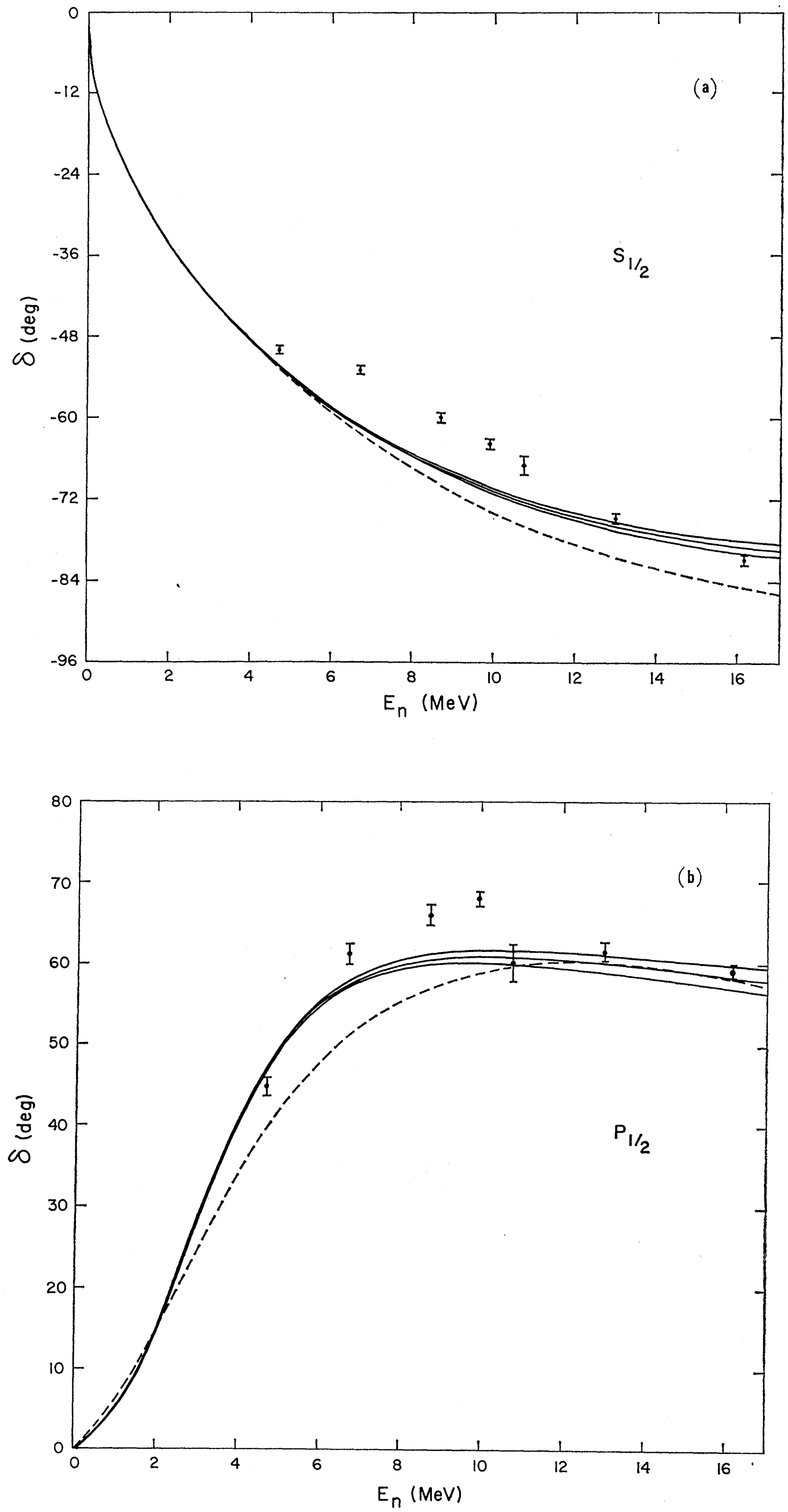

FIG. 8. Solution 18 of Table III (solid curves), HB input (dashed curves), and the latest p-α phase shifts appropriately shifted so that n-α and p-α are at the same c.m. energy.

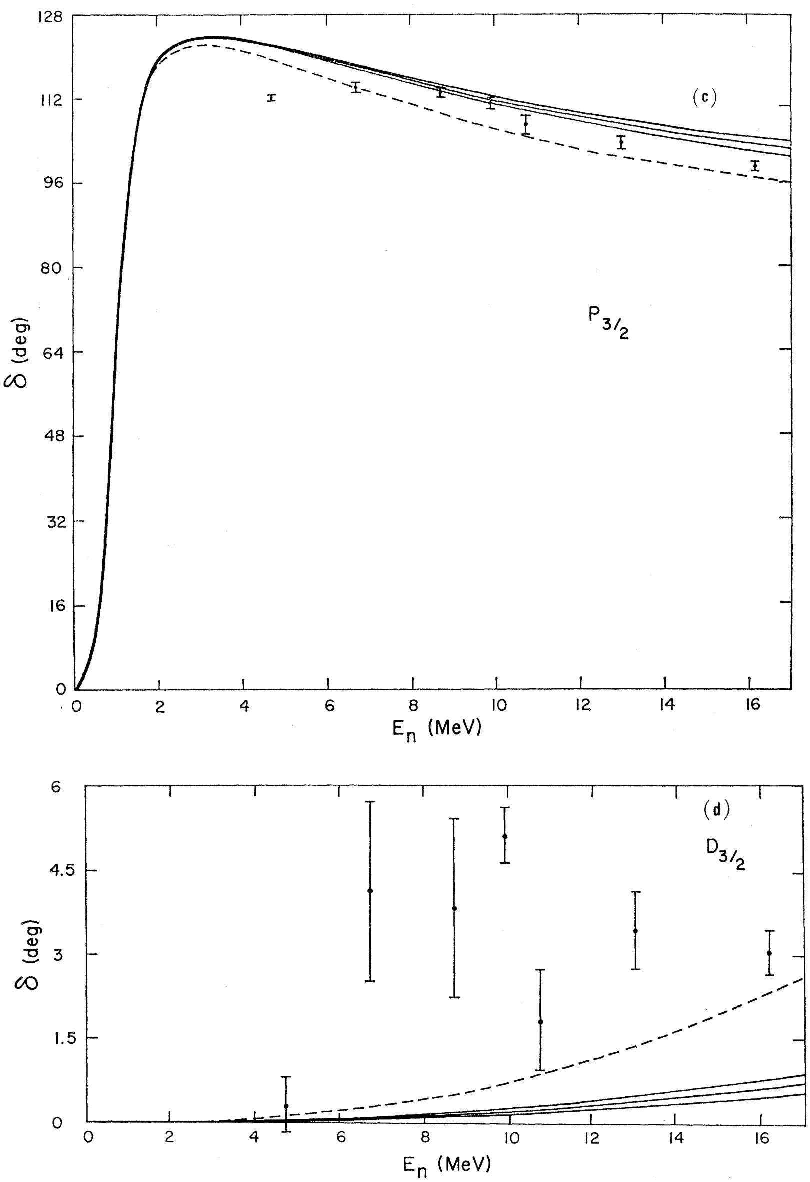

FIG. 8 (*Continued*)

phases do not agree with the HB data at 12, 15, 18, and 20 MeV; particularly at the latter two energies. An example of this disagreement is shown in Fig. 4. Details of the fits are given in Table I. Figures 5 show the curves for s- and p-wave energy-dependent HB phase shifts along with the HB, Duke,[4] and Virginia[7] single-energy phase shifts. We emphasize again that the HB phase shifts were not obtained by a least-squares analysis of the data.

Since the Duke and HB phases agree except for the $P_{1/2}$ phase, we fit the Duke $P_{1/2}$ phases for another set of imput parameters. Other $P_{1/2}$ phase-shift behaviors are tried also. Table II lists the different $P_{1/2}$ phase behaviors and corresponding energy-dependent parameters that we used.

[7] See Ref. D15 in the Appendix.

VI. RESULTS

A. Energy-Dependent Analyses

In every attempt to fit the entire 0–20-MeV data set, high χ^2's were obtained. Much of the excess χ^2 derives from data from 17 to 20 MeV. Because of this and the fact that the HB data and phase shifts do not agree at 18 and 20 MeV, we restricted our analyses to the 0–16.4-MeV range, 16.4 MeV being the highest elastic energy at which polarization data are available.

Table III contains some information about the vari-

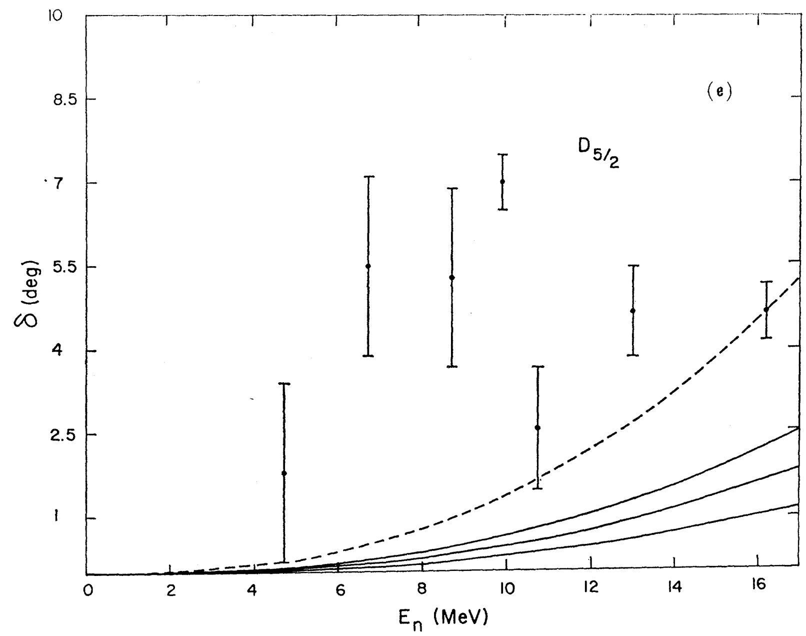

FIG. 8 (*Continued*)

ous 0–16.4 MeV energy-dependent analyses. The HB input (solution 1) did not yield as good a fit as did the modified $P_{1/2}$ HB inputs (solutions 2 and 3). Solutions 2 and 3 were then investigated with regard to the necessity for F and D waves (solutions 5–10). It was determined that the data can be fit as well with s and p waves as with SPDF waves or SPD waves. The first ten solutions were then examined for data that were consistently badly fitted. By this means, 17 total cross-section values were eliminated and the HB2 and HB3 SP and SPD solutions were analyzed again with the reduced data set (solutions 11–14). Solution 11 is plotted in Fig. 6 along with some of the HB and Duke single-energy phases. Also, the HB input was tried again, but it still yielded a higher χ^2 than HB2 or HB3 (solutions 15 and 16).

TABLE IV. Energy-dependent parameters for solution 18 of Table III.

l_{2J}	n	γ_n	$\Delta\gamma_n$ [a]
S_1	0	-0.8390	0.0020
	1	0.06220	0.00047
	2	-0.001686	0.000089
P_1	0	0.5965	0.0070
	1	-0.0980	0.0027
	2	0.01300	0.00040
	3	-0.000162	0.000033
P_3	0	0.12396	0.00044
	1	-0.10381	0.00065
	2	0.00432	0.000022
	3	-0.000054	0.000021
D_3	0	540	140
D_5	0	189	67
F_5	0	5700	10 800
F_7	0	3300	1 900

[a] $\Delta\gamma_n$ is the change in γ_n that changes χ^2 by 1 when all other parameters are searched.

After these energy-dependent analyses and most of the single-energy analyses described below were completed, we learned that Broste and Simmons at Los Alamos Scientific Laboratory had measured the polarization at 11 MeV.[8] We included this new data in the reduced data set and reanalyzed with HB, HB2, and HB3 as input. Again the latter two prevail (see solutions 17–19), and the HB2 (solution 18) and HB3 (solution 19) solutions are essentially the same solution. Solution 18 is plotted in Fig. 7 along with HB input and some of the single-energy solutions described below. The energy-dependent parameters for solution 18 are listed in Table IV.

B. Single-Energy Analyses

Energies at which several values of neutron polarization are available are 1.015, 2, 2.44, 6, 10, 11, and 16.4 MeV. Since differential and total cross sections are available at or very near these energies, we did "single-energy" analyses at these energies with the following energy parameterization:

$$\delta(E_n)=\delta(E_n')+\Delta(E_n-E_n'),$$

where $\delta(E_n')$ is the value of the phase shift at energy $E_n=E_n'$. The slope Δ was kept constant while $\delta(E_n')$

[8] See Ref. P8 in the Appendix.

TABLE V. Single-energy-analyses results.[a]

(A) Energy—1.015 MeV (1.008–1.023)
Data—53 data [$40\sigma(\theta)$, $12P(\theta)$, $1\sigma_T$]

Phase \ Solution		HB	√ HB+D Waves	Solution No. 11 of Table III
$S_{1/2}$:	in	−24	−24	−23.96
	out	−24.00±0.40	−25.27±0.73	−24.00±0.40
	slope	−12.3	−12.3	−12.1
$P_{1/2}$:	in	6	6	4.770
	out	4.65±0.19	4.18±0.24	4.66±0.19
	slope	8.2	8.2	7.7
$P_{3/2}$:	in	61	61	62.76
	out	62.97±0.33	62.22±0.42	62.97±0.33
	slope	135	135	133
$D_{3/2}$:	in		0	
	out		−0.43±0.13	
	slope		0	
$D_{5/2}$:	in		0	
	out		−0.70±0.31	
	slope		0	
χ^2	in	763	763	120
	norm[b]	275	275	71.0
	out	69.0	47.0	68.9
Norm[c]	$\sigma(\theta)$	1.0104	1.0138	1.0043
	$P(\theta)$	1.0043	1.0018	1.0043

(B) Energy—2 MeV (1.961–2)
Data—48 data [$36\sigma(\theta)$, $10P(\theta)$, $2\sigma_T$]

Phase \ Solution		HB	√ HB+D Waves	Solution No. 11 of Table III
$S_{1/2}$:	in	−34	−34	−33.959
	out	−34.64±0.39	−34.09±0.48	−34.64±0.40
	slope	−8.92	−8.92	−8.77
$P_{1/2}$:	in	15	15	14.88
	out	15.06±0.75	15.44±0.84	15.12±0.74
	slope	9.56	9.56	12.4
$P_{3/2}$:	in	118	118	119.038
	out	118.91±0.46	118.77±0.46	119.03±0.46
	slope	10.3	10.3	13.9
$D_{3/2}$:	in		0	
	out		0.97±0.36	
	slope		0	
$D_{5/2}$:	in		0	
	out		0.18±0.12	
	slope		0	
χ^2	in	139	139	71.2
	norm[b]	124	124	61.3
	out	39.6	30.1	39.5
Norm[c]	$\sigma(\theta)$	1.0011	0.9949	1.0010
	$P(\theta)$	1.0138	0.9903	1.0137

(C) Energy—2.44 MeV (2.406–2.454)
Data—53 data [$40\sigma(\theta)$, $12P(\theta)$, $1\sigma_T$]

Phase \ Solution		HB	√ HB+D Waves	Solution No. 11 of Table III
$S_{1/2}$:	in	−38	−38	−37.60
	out	−38.24±0.30	−37.85±0.59	−38.26±0.30
	slope	−8.00	−8.00	−7.88

TABLE V (*Continued*)

$P_{1/2}$:	in	20	20	20.63
	out	20.80±0.26	20.77±0.38	20.80±0.26
	slope	9.57	9.57	13.5
$P_{3/2}$:	in	120	120	122.70
	out	122.16±0.35	122.42±0.54	122.14±0.35
	slope	3.07	3.07	4.69
$D_{3/2}$:	in		0	
	out		0.18±0.15	
	slope		0	
$D_{5/2}$:	in		0	
	out		−0.09±0.25	
	slope		0	
χ^2	in	428	428	84.9
	norm[b]	268	268	53.8
	out	48.0	45.6	48.0
Norm[c]	$\sigma(\theta)$	0.9981	1.0051	0.9978
	$P(\theta)$	1.0087	1.0089	1.0087

(D) Energy—6 MeV (5.988–6.06)
Data—71 data [$60\sigma(\theta)$, $10P(\theta)$, $1\sigma_T$]

Phase \ Solution		(1) HB	HB+D waves	(2) Solution No. 11 of Table III	√ (2)+D waves
$S_{1/2}$:	in	−59	−59	−58.11	−58.16
	out	−60.37±0.17	−60.07±0.62	−58.16±0.16	−58.28±0.52
	slope	−4.33	−4.33	−4.19	−4.19
$P_{1/2}$:	in	47	47	55.56	55.86
	out	50.40±0.19	50.8±1.1	55.86±0.17	55.9±0.89
	slope	5.08	5.08	4.14	4.14
$P_{3/2}$:	in	115	115	119.56	119.59
	out	114.81±0.15	115.7±0.70	119.59±0.13	119.73±0.59
	slope	−2.83	−2.83	−0.667	−0.667
$D_{3/2}$:	in		0		0
	out		−0.37±0.48		−0.14±0.38
	slope		0		0
$D_{5/2}$:	in		0		0
	out		−0.41±0.31		−0.07±0.23
	slope		0		0
χ^2	in	773	773	463	447
	norm[b]	723	723	116	112
	out	135	127	112	111
Norm[c]	$\sigma(\theta)$	0.9969	1.0050	1.0237	1.0248
	$P(\theta)$	1.0233	1.0153	0.9880	0.9872

(E) Energy—10 MeV (10–11)
Data—51 data [$22\sigma(\theta)$, $7P(\theta)$ @ 10 MeV, $21P(\theta)$ @ 11 MeV, $1\sigma_T$]

Phase \ Solution		(1) HB	(2) HB SPD	(3) √ HBSP	Solution No. 15	(3)+D waves
$S_{1/2}$:	in	−74	−74	−74	−70.60	−71.7
	out	−71.8±1.1	−69.6±1.4	−71.7±1.1	−71.7±1.1	−71.9±5.4
	slope	−2.5	−2.5	−2.5	−2.2	−2.5
$P_{1/2}$:	in	60	60	60	61.24	57.8
	out	58.4±1.5	64.9±3.1	57.8±1.2	58.0±1.2	58±17
	slope	0.5	0.5	0.5	−0.0143	0.5
$P_{3/2}$:	in	107	107	107	112.25	108.3
	out	108.5±1.3	111.9±1.7	108.3±1.2	108.1±1.2	108.2±9.8
	slope	−2.	−2.	−2.	−1.37	−2.

TABLE V (*Continued*)

$D_{3/2}$:	in		0			0
	out		2.8±1.4			−0.12±6.7
	slope		0			0
$D_{5/2}$:	in	2	2			0
	out	0.31±1.44	3.7±1.6			0.13±8.2
	slope	0	0			0
χ^2	in	92.4	92.4	121	102.7	65.0
	norm[b]	81.9	81.9	108	86.5	
	out	59.8	58.1	60.3	65.2	59.9
Norm[d]	$\sigma(\theta)$	1.0063	1.0031	1.0072	1.0069	1.0061
	$P(\theta)$ 10 MeV	1.0008	1.0169	0.9994	1.0002	1.0008
	$P(\theta)$ 11 MeV[c]	1.0156	1.0346	1.0127	1.0068	1.0155
	$P(\theta)$ 11 MeV	1.0179	1.0411	1.0203	1.0119	1.0182

(F) Energy—12 MeV (11–12.38)
Data—41 data [$18\sigma(\theta)$, $21P(\theta)$, $2\sigma_T$]

Solution / Phase		(1) Late norm HB	(2) HB SP	(3) Solution No. 11 of Table III	√ (3)+D waves
$S_{1/2}$:	in	−79	−79	−74.	−75.1
	out	−66.6±1.3	−75.0±1.2	−75.1±1.2	−68.1±1.4
	slope	−2.5	−2.5	−2.2	−2.2
$P_{1/2}$:	in	61	61	61	56.7
	out	75.2±2.0	56.7±1.3	56.7±1.3	73.4±2.1
	slope	0.5	0.5	−0.01	−0.01
$P_{3/2}$:	in	103	103	109	105.3
	out	114.35±0.89	105.2±1.3	105.3±1.3	113.7±0.99
	slope	−2.	−2.	−1.4	−1.4
$D_{3/2}$:	in	1			0
	out	7.93±0.88			6.98±0.94
	slope	0.5			0
$D_{5/2}$:	in	2			0
	out	9.26±0.92			8.6±1.0
	slope	0			0
χ^2	in	212	274	162	125
	norm[b]	···	···	···	···
	out	51.6	74.2	63.3	43.8
Norm[c]	$\sigma(\theta)$	1.0559	1.0637	1.0636	1.0553
		1.0866	1.0046	1.0102	1.0807
	$P(\theta)$	1.0917	1.0027	1.0116	1.0886

(G) Energy—16.4 MeV (16.4 only; therefore, no slopes are required)
Data—27 data [$19\sigma(\theta)$, $8P(\theta)$, $0\sigma_T$]

Solution / Phase		(1) HB	(2) √ HB SPD	(3) Solution No. 11 of Table III	(4) (3)+D waves	HB SP	Solution No. 13	(4)+F waves
$S_{1/2}$:	in	−85	−85	−78.83	−83.3	−85	−78.96	−86
	out	−105±12	−100.3±4.4	−83.3±4.9	−86.±11	−85.2±5.2	−100.3±4.4	−107±13
$P_{1/2}$:	in	57.5	57.5	59.26	51.6	57.5	59.34	56
	out	42±11	47.3±4.8	51.6±4.1	56±15	50.3±4.2	47.3±4.8	41±12
$P_{3/2}$:	in	96.5	96.5	105.15	98.0	96.5	105.20	100
	out	88.2±9.0	91.4±5.2	98.0±4.5	100±10	96.3±4.6	91.4±5.2	87.3±9.2
$D_{3/2}$:	in	2	2		0		−1.296	3.5
	out	1.4±4.6	4.2±1.7		3.5±11		4.2±1.7	0.9±4.6

TABLE V (*Continued*)

$D_{5/2}$:	in	5	5		0		−0.350	3.8
	out	2.2±5.1	5.7±2.7		3.8±14		5.7±2.7	1.6±4.9
$F_{5/2}$:	in	1						0
	out	−1.2±2.3						−1.5±2.3
$F_{7/2}$:	in	1						0
	out	−3.1±4.3						−3.6±4.3
χ^2	in	26.4	25.9	39.8	19.6	29.6	43.7	17.1
	norm[b]	25.1	24.7	16.3	12.8	23.6	18.5	12.2
	out	6.43	7.12	12.8	12.3	12.7	7.12	6.52
Norm[c]	$\sigma(\theta)$	1.0005	1.0016	0.9793	0.9790	0.9798	1.0015	1.0007
	$P(\theta)$	1.0058	1.0388	0.9349	0.9469	0.9469	1.0387	1.0041

[a] Check mark indicates solution plotted in Fig .7.
[b] χ^2 after renormalization of angular data but before searching the parameters.
[c] Factor the search code chose to divide the data by for the best fit.
[d] There are two LASL data sets at 11 MeV. The smaller set is listed first.

was varied. The values for Δ and input values for $\delta(E_n')$ were usually HB or solution 11 of Table III.

The results of the single-energy analyses are given in Table V. As with the energy-dependent analyses, inclusion of D or F waves usually did not improve the fits. The best solutions have a check mark above them in Table V and are plotted along with HB input and solution 18 of Table III in Fig. 7. It is obvious that our energy-dependent solution is a compromise among the erratic single-energy solutions at 10, 12, and 16.4 MeV.

VII. CONCLUSIONS

From 3 to 10 MeV, the $P_{1/2}$ phase appears to be larger than the values given by HB. However, we were not able to get a good χ^2 for the 6-MeV single-energy analysis. It would be helpful to have some very precise polarization data in this energy range *at* energies where recent differential cross sections are available

There appear to be inconsistencies among the data above 10 MeV. Up to 16.4 MeV our energy-dependent solution smoothes out these inconsistencies with a reasonable χ^2. Our $S_{1/2}$ and $P_{3/2}$ phases are larger than HB from 10 to 16.4 MeV. Up to 20 MeV we get χ^2's of about 4000 for 1460 data, about 1500 of it coming from 50 data between 16.4 and 20 MeV. There are no polarization data in this range. Some very careful measurements of differential cross sections and polarization *at the same energies* are needed from 10 to 20 MeV.

We are not able to make any statements about D and F waves other than that the D waves tend to be positive.

In the Introduction, we mentioned that n-α and p-α scattering should be almost identical. We now examine them together by comparing our n-α phase shifts with the latest elastic p-α phase shifts.[9] In Fig. 8 are plotted these p-α phases along with our solution 18 of Table III and the HB input. We have shifted the p-α phases down by 1.29 MeV in order that the n-α and p-α systems be at the same c.m. energy. There appear to be large inconsistencies among the p-α phases themselves. However, they seem to be in better agreement with our solution than with HB. (Remember that we cannot determine D waves as judged by lack of improvement in χ^2, even though we plot our values here.) We are presently analyzing the p-α data with our energy-dependent parameterization.

[9] See the last two articles of Ref. 1.

After this report was written we were informed by J. E. Simmons of Los Alamos Scientific Laboratory that we had overlooked some polarization data at 12, 16.2, and 20.7 MeV (see the Appendix, P1A and P5A) because the article titles did not indicate that n-α polarization data were reported in them. We plotted our solution 18 of Table III versus this "new" data and found that the agreement was close. Then we reran the 12-MeV (Table V, part f) and 16.4-MeV (Table V, part g) single-energy-analyses best solution (check marked in the two tables) with this new "data" with the following results.

12 MeV:

$$S_{1/2}=-68.6\pm1.3,$$
$$P_{1/2}=72.5\pm2.0,$$
$$P_{3/2}=113.5\pm1.0,$$
$$D_{3/2}=6.4\pm0.9,$$
$$D_{5/2}=8.1\pm1.0,$$
$$\text{No. of data}=47, \qquad \chi^2=54.1.$$

The change from Table V, part f is well within the errors.

16.4 MeV:

$$S_{1/2}=-101.8\pm3.6,$$
$$P_{1/2}=44.8\pm4.0,$$
$$P_{3/2}=89.9\pm4.8,$$
$$D_{3/2}=3.0\pm1.4,$$
$$D_{5/2}=4.1\pm2.3,$$
$$\text{No. of data}=38, \qquad \chi^2=22.7.$$

The change from Table V, part g is well within the errors. Therefore, we conclude that this neglected data cannot affect our energy-dependent solution very much. We shall rerun that solution with all available data when more data become available.

We have facilities to plot observables at any energy and angle with errors as predicted by our solution, and would be glad to do so upon request. Also, the listing of the complete data set and the data selection used in our analyses is available.

ACKNOWLEDGMENTS

Dr. Brian DeFacio contributed to the early phases of this work. We are grateful to Dr. H. H. Barschall and Dr. B. Hoop, Jr., for answering our questions and supplying tabulated data. Also, R. L. Walter gave us considerable help with the polarization data. Dr. J. E. Simmons of Los Alamos Scientific Laboratory was very helpful in supplying comments and new data. The authors are grateful for 1968 summer faculty positions at Lawrence Radiation Laboratory, Livermore, Calif. while this work was in progress.

APPENDIX: DATA REFERENCES

Total cross sections:

T1. S. Bashkin, F. P. Mooring, and B. Petree, Phys. Rev. **82**, 378 (1951)—0.04–4.9 MeV (36 energies) (data in graph form).

T2. R. B. Day and R. L. Henkel, Phys. Rev. **92**, 358 (1953)—17.97, 19., and 20.07 MeV [Same results as given in Battat *et al.*, Nucl. Phys. **12**, 291 (1959)].

T3. *PR P.* 28 (1955) Unpublished Chalk River data [tabulated in R. J. Howerton, W. J. Cahill, K. L. Hill, D. W. Thompson, and S. T. Perkins, Lawrence Radiation Laboratory, Livermore, Report No. UCRL 50400, 1968 (unpublished)]—47.5 and 88 MeV.

T4. M. E. Battat, R. O. Bondelid, J. H. Coon, L. Cranberg, R. B. Day, F. Edeskuty, A. H. Frentrop, R. L. Henkel, R. L. Mills, R. A. Nobles, J. E. Perry, D. D. Phillips, T. R. Roberts, and S. G. Sydoriak, Nucl. Phys. **12**, 291 (1959)—0.94, 1.5, 1.98, 2.49, 2.99, 4.95, 5.52, 6.06, 6.59, 7.1, 12.35, 12.65, 13.13, 14.1, 14.14, 15.18, 17.62, 17.97, 19, and 20.07 MeV.

T5. F. J. Vaughn, W. L. Imhof, R. G. Johnson, and M. Walt, Phys. Rev. **118**, 683 (1960); F. J. Vaughn (private communication)—0.122–6.227 MeV and 12.079–19.769 MeV (140 energies).

T6. S. M. Austin, H. H. Barschall, and R. E. Shamu, Phys. Rev. **126**, 1532 (1962)—6.99, 8.03, 10.07 and 12.01 MeV.

T7. R. Genin, H. Beil, C. Signarbieux, P. Carlos, R. Joly, and M. Ribrag, J. Phys. Radium **24**, 21 (1963) [tabulated in R. J. Howerton *et al.*, Lawrence Radiation Laboratory, Livermore, Report No. UCRL 50400, 1968 (unpublished)]—2.1×10^{-9}–2.51×10^{-8} MeV (24 energies) (data in graph form).

T8. R. E. Shamu and J. G. Jenkin, Phys. Rev. **135**, B99 (1964)—20–29 MeV (26 energies).

T9. D. F. Measday and J. N. Palmieri, Nucl. Phys. **85**, 129 (1966)—77.2, 88.2, 110.0, 129.4, and 150.9 MeV.

Differential cross sections:

D1. R. K. Adair, Phys. Rev. **86**, 155 (1952) [tabulated in R. J. Howerton, W. J. Cahill, K. L. Hill, D. W. Thompson, and S. T. Perkins, Lawrence Radiation Laboratory, Livermore, Report No. UCRL 50400, 1968 (unpublished)]—0.4, 0.6, 0.75, 0.865, 1.0, 1.2, 1.4, 1.7, 2, 2.4, and 2.73 MeV (data in graph form).

D2. P. Huber and E. Baldinger, Helv. Phys. Acta **25**, 435 (1952)—3.01, 3.21, 3.5, 3.77, 3.89, 4.0, and 4.14 MeV (data not in a useable form).

D3. J. D. Seagrave, Phys. Rev. **92**, 1222 (1953) [tabulated in R. J. Howerton *et al.*, Lawrence Radiation Laboratory, Livermore, Report No. UCRL 50400, 1968 (unpublished)]—2.61, 4.53, 5.54, 6.5, and 14.3 MeV (data in graph form).

D4. J. R. Smith, Phys. Rev. **95**, 730 (1954)—14.1 MeV (data in graph form).

D5. H. R. Striebel and P. Huber, Helv. Phys. Acta **29**, 67 (1956)—2.61, 2.86, 3.06, 3.24, 3.4, 3.57, 3.68, 3.85, and 4.09 MeV (data not in a useable form).

D6. T. W. Bonner, F. W. Prosser, Jr., and J. Slattery, Phys. Rev. **115**, 398 (1959)—16–23.4 MeV (data not in a useable form).

D7. M. Arnold, P. E. Hodgson, D. F. Shaw, and D. M. Skyrme, Nucl. Phys. **19**, 500 (1960)—60, 100, and 140 MeV.

D8. F. Demanins, G. Pisent, G. Poiani, and C. Villi, Phys. Rev. **125**, 318 (1962)—2.37 and 2.87 MeV (data in form of $\cos\theta$ coefficients).

D9. S. M. Austin, H. H. Barschall, and R. E. Shamu, Phys. Rev. **126**, 1532 (1962)—2.02, 3.02, 4.05, 5.97, 7.96, 10, 12, 14.7, 17.8, 20.9, and 22.3 MeV [superceded by Hoop and Barschall, Nucl. Phys. **83**, 65 (1966)].

D10. R. Malaroda, G. Poiani, and G. Pisent, Phys. Letters **5**, 205 (1963)—14.9 MeV (data not in a useable form).

D11. U. Fasoli and G. Zago, Nuovo Cimento **30**, 1 (1963)—14.1 MeV (data not normalized).

D12. R. E. Shamu and J. G. Jenkin, Phys. Rev. **135**, B99 (1964)—16.4, 20, 21, 21.85, 21.97, 21.99, 22.02, 22.05, 22.07, 22.1, 22.13, 22.15, 22.18, 22.2, 22.23, 22.25, 22.32, 22.37, 22.42, 22.6, and 23.7 MeV [data in form of $P_l(\cos\theta)$ coefficients].

D13. B. Hoop, Jr., and H. H. Barschall, Nucl. Phys. **83**, 65 (1966); B. Hoop, Jr. (private communication); H. H. Barschall (private communication); B. Hoop, Jr., Ph.D. thesis, University of Wisconsin, 1967 (unpublished)—2.02, 3.02, 4.05, 5.97, 8.02, 10, 12.38, 15.05, 17.74, 19.26, 20.91, 21.85, 22., 22.05, 22.1, 22.13, 22.2, 22.26, 22.45, 23.67, 24.66, 25.66, 26.63, 28.56, and 30.71 MeV.

D14. G. L. Morgan and R. L. Walter, Phys. Rev. **168**, 1114 (1968); R. L. Walter (private communication)—0.202, 0.303, 0.402, 0.501, 0.599, 0.704, 0.799, 0.899, 1.008, 1.106, 1.207, 1.306, 1.7, 1.961, 2.2, 2.454, 2.98, 5.028, 5.505, 5.988, 6.523, and 7.013 MeV.

D15. D. Cramer, D. Simmons, and L. Cranberg, University of Virginia, 1968 (unpublished); D. Cramer (private communication)—0.545 and 0.84 MeV.

Polarization:

P1. R. E. White and F. J. M. Farley, Nucl. Phys. **3**, 476 (1957)—3 MeV and 90° c.m.

P1A. I. S. Trostin, V. A. Smotryaev, and I. I. Levintov, Zh. Eksperim.: Teor. Fiz. **41**, 725 (1961) [English transl.: Soviet Physics—JETP **14**, 524 (1962)]—20.7 MeV (90°–150° c.m.).

P2. T. H. May, R. L. Walter, and H. H. Barschall, Nucl. Phys. **45**, 17 (1963)—2.0, 6.0, 10.0, 16.4, and 23.7 MeV. (30°–120° lab). [These data have been recalculated with further corrections by J. R. Sawers, Jr., G. L. Morgan, L. A. Schaller, and R. L. Walter, Phys. Rev. **168**, 1102 (1968) (2 MeV); G. L. Morgan and R. L. Walter, *ibid.* **168**, 1114 (1968) (6 MeV); R. L. Walter (private communication) (10, 16.4, and 23.7 MeV)].

P3. I. I. Levintov, A. V. Miller, and V. N. Shamshev, Nucl. Phys. **3**, 221 (1957)—2.45 and 3.4 MeV (data not in a useable form).

P4. R. B. Perkins and C. Glashausser, Nucl. Phys. **60**, 433 (1964)—23.1 MeV (60°–140° lab).

P5. R. W. Jewell, W. John, J. E. Sherwood, and D. H. White, Phys. Rev. **142**, 687 (1966)—0.262 MeV and 89° c.m.

P5A. F. W. Büsser, F. Niebergall, and G. Söhngen, Nucl. Phys. **88**, 593 (1966)—12 MeV (120°–170° c.m.) and 16.2 MeV (90°–160° c.m.).

P6. U. R. Arifkhanov, N. A. Vlasov, V. V. Davydov, and L. N. Samoilov, Yadern. Fiz. **2**, 239 (1965) [English trans.: Soviet J. Nucl. Phys. **2**, 170 (1966)]—25, 27.8, and 34.1 MeV (47.5°–150° lab)].

P7. J. R. Sawers, Jr., G. L. Morgan, L. A. Schaller, and R. L. Walter, Phys. Rev. **168**, 1102 (1968)—1.015 and 2.44 MeV (30°–140° lab).

P8. W. B. Broste and J. E. Simmons, Los Alamos Scientific Laboratory (private communication)—11 MeV (50°–160° c.m.).